Variability of the Antarctic Coastal Current and its origins

Ismael Núñez-Riboni and Eberhard Fahrbach

Alfred-Wegener-Institut für Polar- und Meeresforschung

General Assembly of the European Geophysical Union. Vienna, Austria. April, 2007.

Introduction

Antarctic Bottom Water (AABW) is supposed to have an important impact on the meridional overturning circulation of the global ocean. This renders AABW to an important element of the thermohaline circulation. About 50 to 70% of the AABW originates in the Weddell Sea.

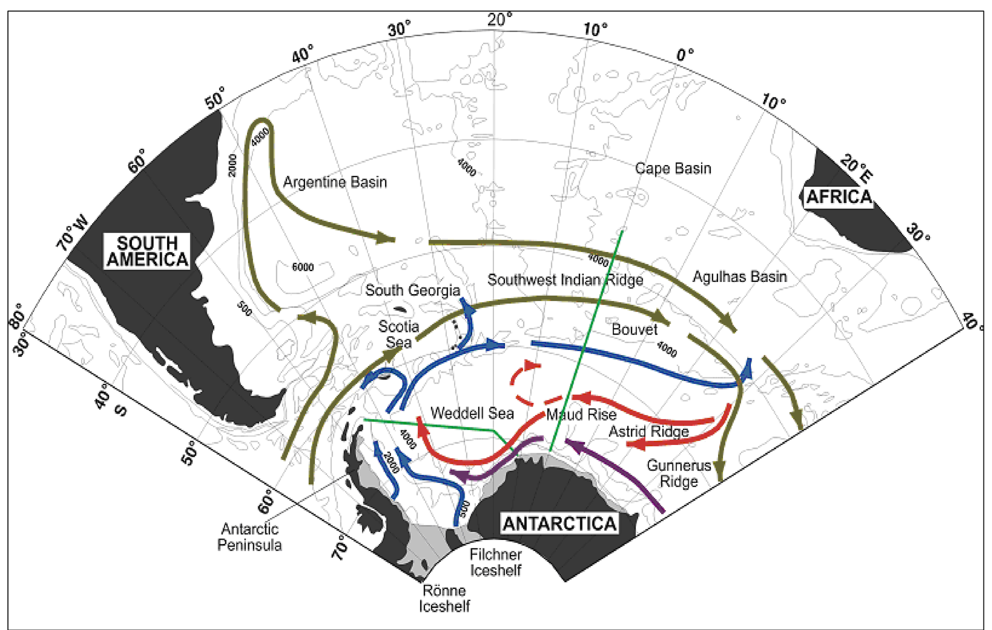

Figure 1. Water mass formation in the Weddell Sea. The mixture of NADW with recently formed AABW in the Antarctic Circumpolar Current (ACC; olive arrows) yields a mixture which enters into the Weddell gyre: Warm Deep Water (WDW; red arrows). WDW is transported in the southern limb of the gyre and contributes to the formation of Western Shelf Water (WSW) which, by mixing with WDW, can sink along the Antarctic continental slope to form Weddell Sea Bottom Water (WSBW). WSBW flows to the northwest (blue arrows) and mixes again to form Weddell Sea Deep Water (WSDW) which then can leave the Weddell Sea.

The Antarctic Coastal Current (ACoC; magenta arrows) surrounds Antarctica flowing westwards, counter to the ACC. It is the major transport way to carry WDW in the deep and bottom water formation area in the southwestern Weddell Sea. The present study attempts to quantify the influence of the wind and ice concentration on the ACoC, as well as to clarify the role that temporal and spatial variations of the current play in the formation of AABW in the Weddell Sea.

Data description. To measure the fluctuations in the ACoC, two moorings (AWI-232 and AWI-233) were maintained on the prime meridian (cyan line in Figure 1) from 1996 to 2005. Wind time series are from the European Center for Medium-Range Weather Forecast (ECMWF). Hydrographic data were taken on the deployment cruises of RV-Polarstern. There are available nine CTD sections spanning from 1992 to 2005. Sea ice concentration was obtained from the final data set of sea ice concentrations from passive microwave data of the Nimbus-7 Scanning Multichannel Microwave Radiometer (SMMR) and the Special Sensor Microwave/Imager (SSM/I) of the Defense Meteorological Satellite Program (USA).

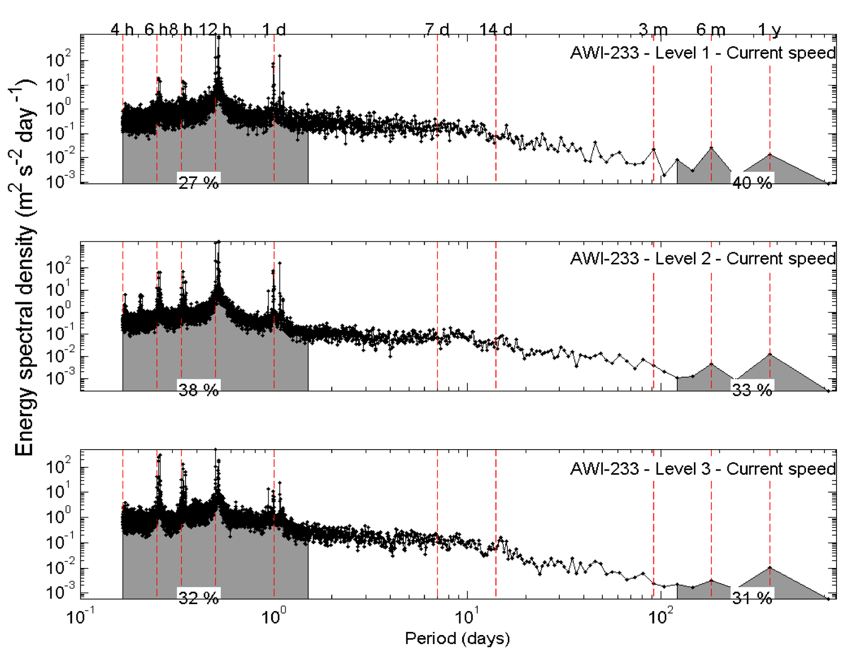

Figure 2. Energy spectral density of (from upper to lower panel) wind, ice concentration, and the three depth levels of AWI-233. Shaded areas represents percentages of the annual variability. Vertical lines indicate maxima.

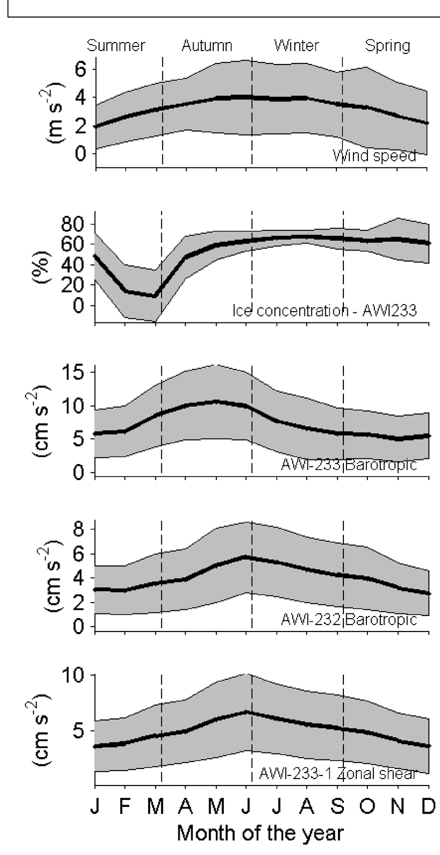

Figure 3. Composite of minimum atmospheric pressure, wind, ice concentration, barotropic component of AWI-233, barotropic component of AWI-232 and surface zonal shear of AWI-233. The shaded areas are the unbiased standard deviations.

Results and conclusions

2. The low frequency fluctuations of the ACoC are mostly generated by the semi-annual and annual components of the wind and the ice (Figs. 2). These components span together ca. 10% of the variability.
3. Wind and ice concentration influence the seasonality of both the barotropic and baroclinic components of the current (Figure 3).
4. The baroclinic core of the ACoC (Fig. 4) is set through heat gain/loss and ice melting/formation, which influence the horizontal density gradient between Shelf Water and Surface/Winter Water (Figs. 5 and 6).

Objectives

2. Determination of mean current, salinity and temperature fields of the ACoC and their time variability.
3. Estimation of the mean volume, heat and freshwater transport of the ACoC.
4. Identification of the scales and causes of the ACoC's variability and its influence on the deep water properties in the Weddell Sea.

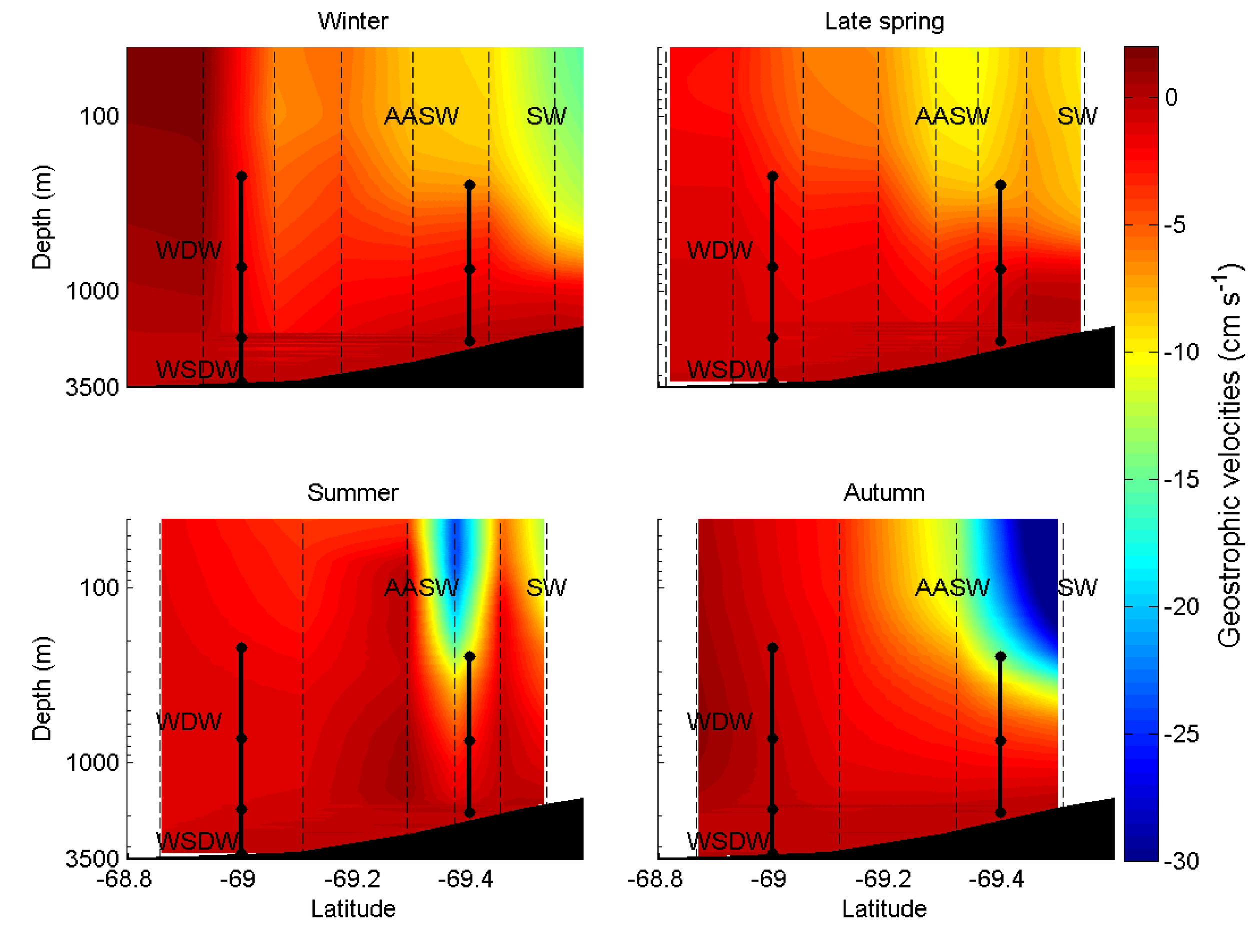

Figure 4. Geostrophic velocities (cm s⁻¹) from hydrographic data of RV-Polarstern for winter (upper left panel), late spring (upper right panel), summer (lower left panel) and autumn (lower right panel). The mean depths of the moored instruments are shown with dots joined with a thick line. Note logarithmic scale for the depth axis.

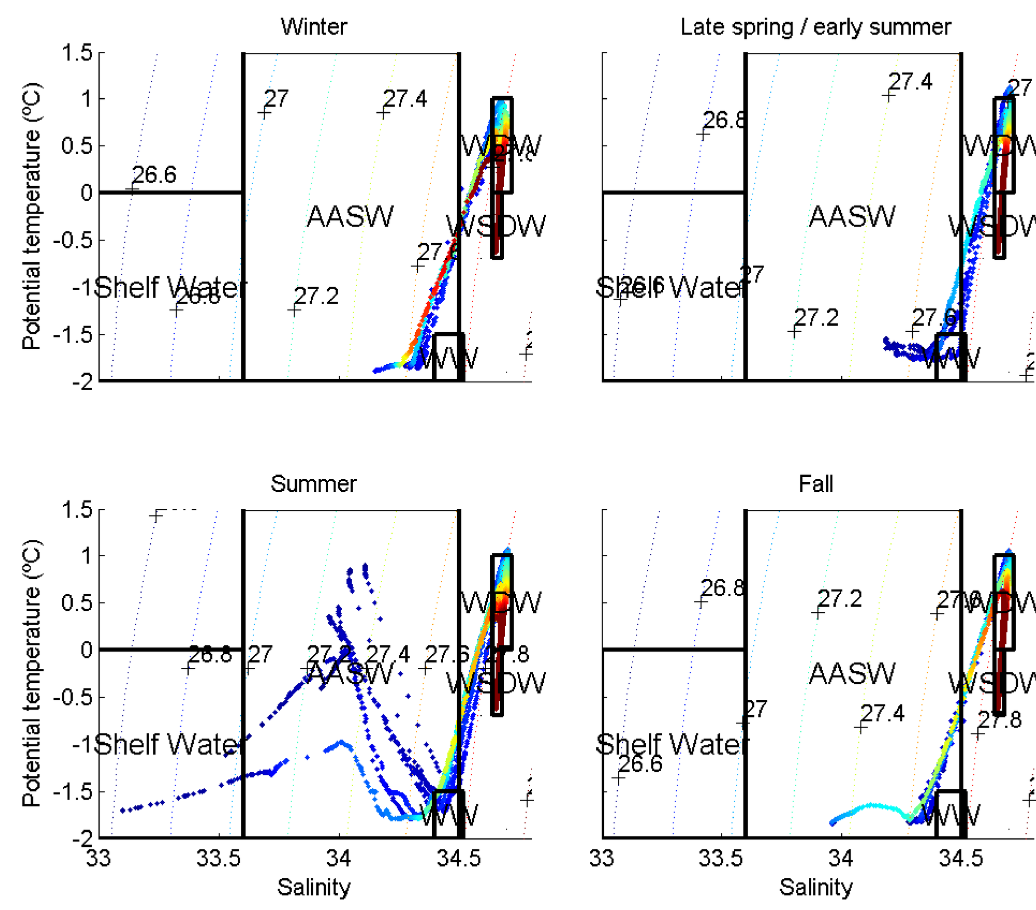

Figure 5. TS diagrams of the same expeditions of Figure 3 (except spring). Water masses are shown within boxes as defined by their hydrographic characteristics. WDW stands for Warm Deep Water, WSDW for Weddell Sea Deep Water and WW for Winter Water.

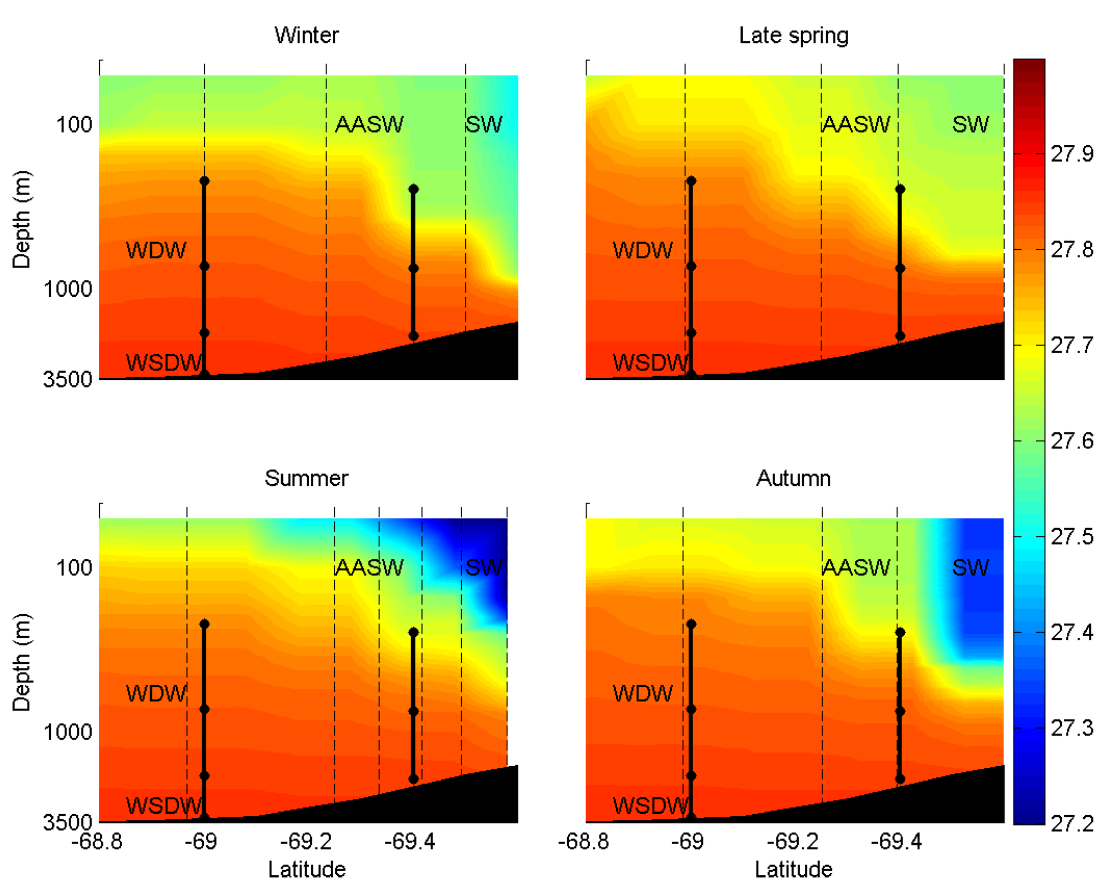

Figure 6. As in Figure 3 but for potential density referred to the surface. Vertical dashed lines denote the positions of the CTD stations.

1. This density gradient is also influenced by the wind, which depresses the isopycnals through onshore Ekman transport and consequent downwelling resulting in vertical current shear according to the thermal wind relation (Fig. 6).
2. Maximum baroclinicity is reached near the surface and the shelf, where 38% of the kinetic energy of the current's fluctuations is baroclinic.
3. Wind and ice concentration have effects on the ACoC that are out of phase because the ice covering the ocean's surface modifies the effect of the wind (Figs. 3 and 8). In consequence the baroclinic and barotropic components of the current are almost in phase (Fig. 3) with maximum speed of the current in autumn.
4. Wind and ice concentration influence the ACoC mainly through their annual component (Fig. 7).
5. Linear trends of the wind's and the current's speed suggest deceleration (not shown) but are not significant at the present state of observation. To determine if the trends could become significant, it is imperative to extend the observation period for 6 more years.

Outlook

To understand the influence of the ACoC's variability on the properties and formation of deep and bottom water, time dependent transports will be estimated and a correlation with historical hydrographic properties of deep and bottom water in the Weddell Sea will be searched.

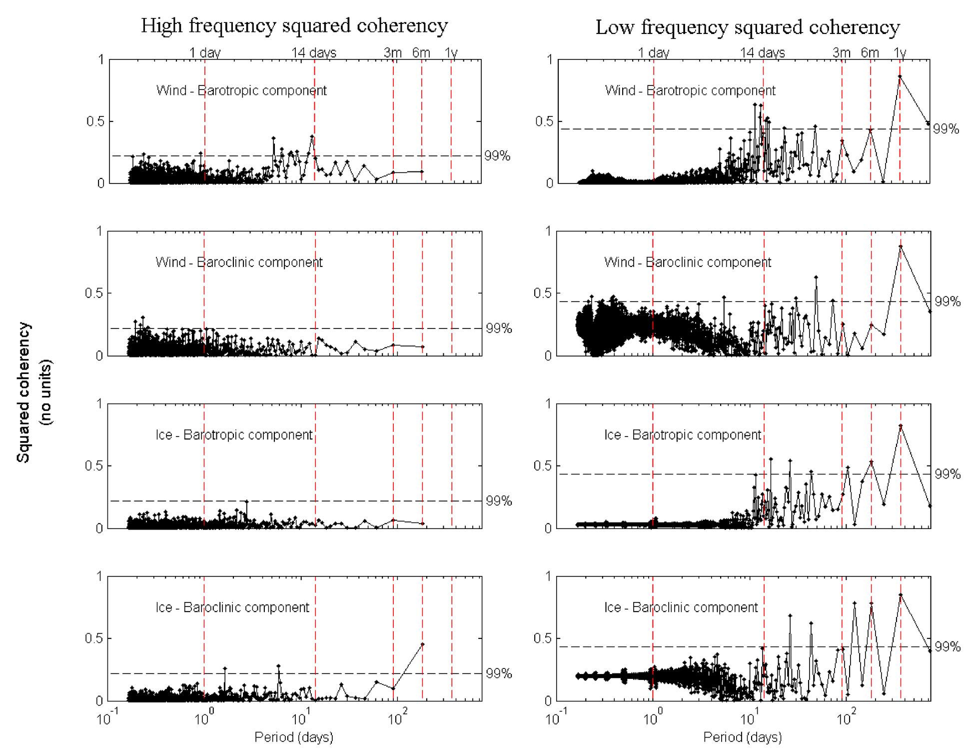

Figure 7. Squared coherencies (no units) between: wind and barotropic component of the ACoC, wind and baroclinic component, ice concentration and barotropic component, as well as ice concentration and baroclinic component. Left (right) panels show the coherency for the high (low) frequency band. The current components correspond to AWI-233 (shallow level, in the case of the baroclinic one).

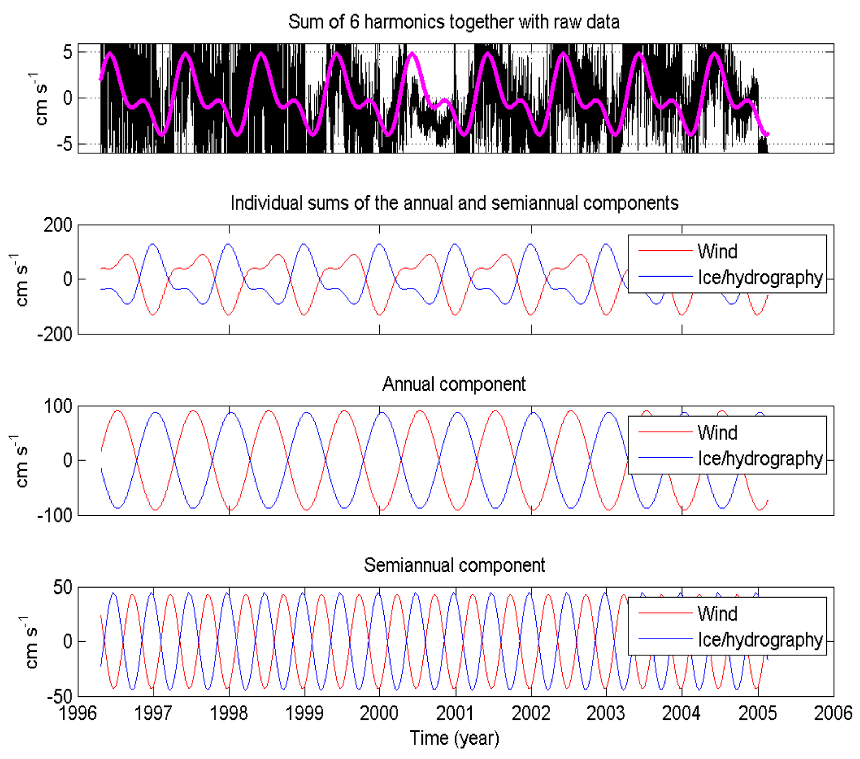

Figure 8. Decomposition of the time series of AWI-233-1 in two annual and two semiannual harmonics, for which the phases were obtained from time series of wind and ice, and the amplitudes from the current meter measurements. Upper panel: the sum of the four harmonics (magenta thick line) superimposed to raw data (black line). Second panel: individual sums of semiannual and annual harmonics. Third panel: the annual component of wind (red) and ice (blue). Lower panel: the semiannual harmonics.

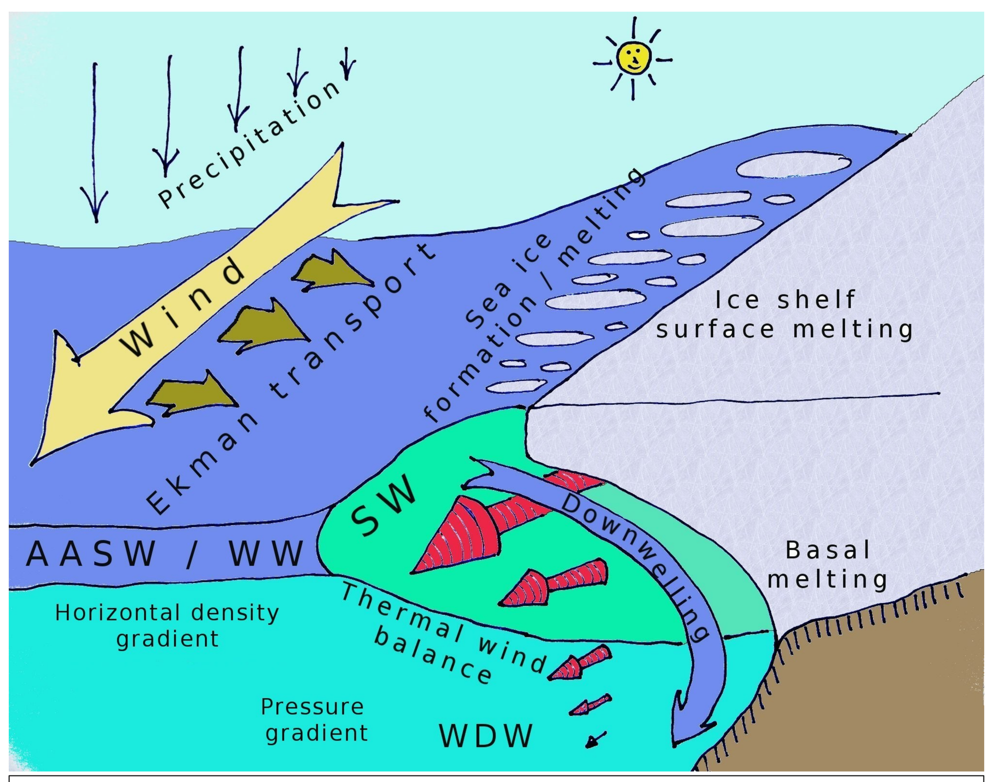

Figure 9. Diagram of the driving mechanisms of the ACoC (red arrows) amd its annual variability. Acronyms like in fig. 4.

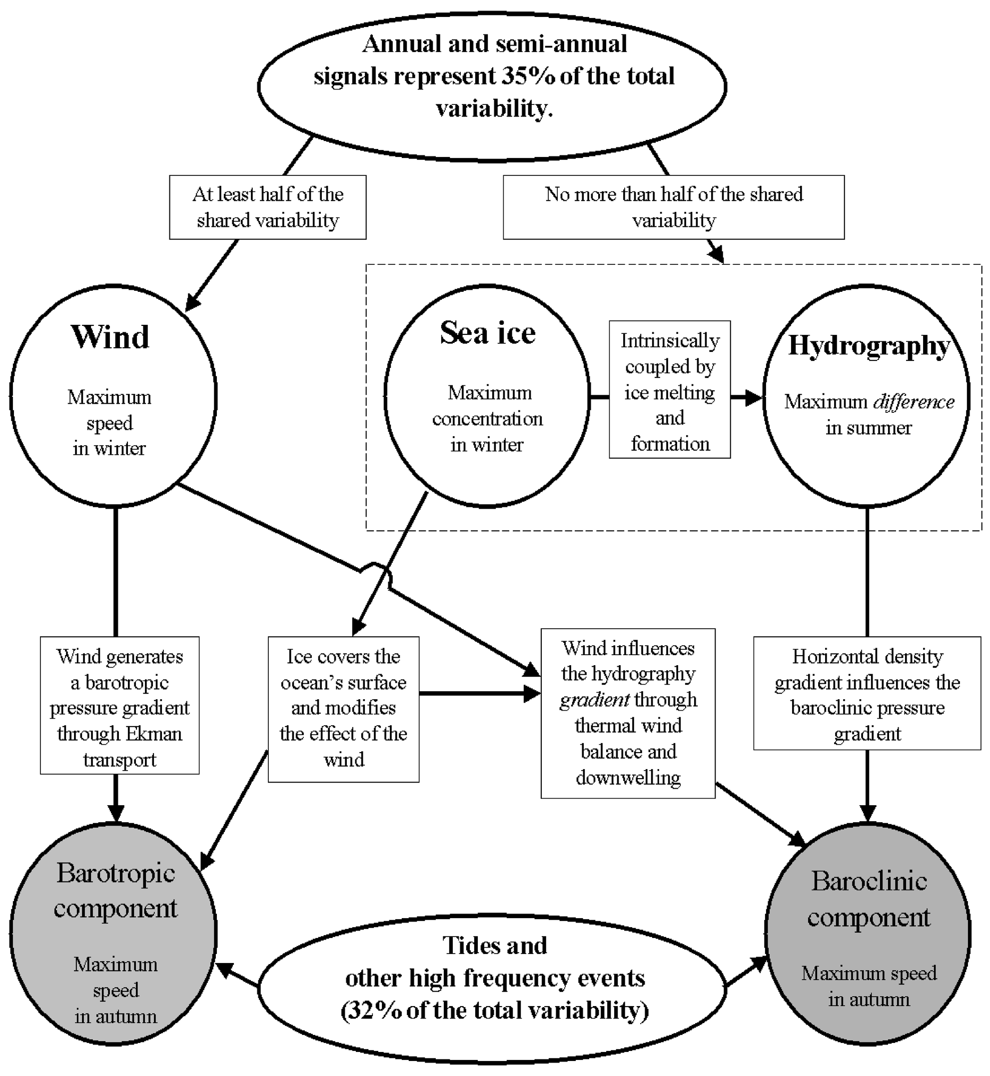

Figure 10. Conceptual map of the driving mechanisms of the ACoC and their mutual interaction.

Acknowledgements

The kind collaboration of Gerd Rohardt, Olaf Klatt, Dmitry Sidorenko, Gert König-Langlo, Angelika Humbert, Ulrike Wacker and Wolfgang Dierking is highly appreciated.